Nonlinear MHD and Energetic Particle Modes in Stellarators

H.R. Strauss
New York University, New York, New York
G. Y. Fu, W. Park, J. Breslau
Princeton University Plasma Physics Laboratory, Princeton, New Jersey
L.E. Sugiyama
Massachusetts Institute of Technology, Cambridge, Massachusetts

Abstract. The M3D (Multi-level 3D) project carries out simulation studies of plasmas using multiple levels of physics, geometry, and grid models. The M3D code has been applied to ideal, resistive, two fluid, and hybrid simulations of compact quasi axisymmetric stellarators. When β exceeds a threshold, moderate toroidal mode number ($n \sim 10$) modes grow exponentially. The β limits are significantly higher than the infinite mode number ballooning limits. In the presence of resistivity, these modes occur well below the ideal limit. Their growth rate scaling with resistivity is similar to tearing modes. At low resistivity, the modes couple to resistive interchanges, which are unstable in most stellarators. Two fluid simulations with M3D show that resistive modes can be stabilized by diamagnetic drift. The two fluid computations are done with a realistic value of the Hall parameter, the ratio of ion skin depth to major radius. Hybrid gyrokinetic simulations with energetic particles indicate that global shear Alfvén TAE - like modes can be destabilized in stellarators. Computations in a two - period compact stellarator obtained a predominantly $n = 1$ toroidal mode with the expected TAE frequency. It is found that TAE modes are more stable in the two - period compact stellarator than in a tokamak with the same q and pressure profiles. The M3D initial value code combines a two dimensional unstructured mesh with finite element discretization in poloidal planes, and fourth order finite differencing in the toroidal direction.

I. Introduction

The M3D (Multi-level 3D) project [1, 2] carries out simulation studies of plasmas using multiple levels of physics, geometry, and grid models. The M3D code has been applied to ideal, resistive, two fluid, and hybrid simulations of compact quasi axisymmetric stellarators. For β above a threshold, ideal MHD low mode number ballooning - like modes appear. In the presence of resistivity, these modes occur well below the ideal limit. Their growth rate scaling with resistivity is similar to tearing modes. Stellarators tend to be resistive interchange unstable, so the resistive modes are not stabilized at small resistivity, as in tokamaks.

Two fluid simulations indicate that the resistive modes are stabilized by diamagnetic drifts. This might account for the lack of experimental evidence of these modes. The two fluid simulations were done with a realistic value of the Hall parameter, which determines the speed of the diamagnetic drift relative to the Alfvén speed.

Hybrid simulations with energetic particles indicate that global shear Alfvén TAE - like modes can be destabilized in stellarators. A sequence of equilibria was studied, with the

amount of three dimensional distortion varying smoothly from no distortion (tokamak) to full three dimensional distortion (stellarator). The rotational transform and pressure was the same for all equilibria in the sequence. It was found that the TAE growth rate was reduced by increasing the three dimensional distortion.

M3D combines a two dimensional unstructured mesh with finite element discretization in poloidal planes [3], and fourth order finite differencing in the toroidal direction. The code is parallelized and runs on both shared and distributed memory computers. Parallelization makes use of both poloidal and poloidal domain decomposition, with each processor holding only a part of the mesh points. Extensive use is made of the PETSc [4] library. Equilibria from the VMEC code [5] are used to construct the M3D grid, and initialize the magnetic field and pressure. VMEC outputs flux surface coordinates in the form $R(s,\theta,\phi), Z(s,\theta,\phi)$ where s is a flux surface label. This is used by M3D to generate a mesh aligned with the VMEC flux surfaces. This mesh is fixed during a computation. VMEC also supplies the toroidal magnetic field B_ϕ, toroidal current J_ϕ, and pressure p. These quantities suffice to initialize M3D.

II. Ideal Equilibrium and Stability

To obtain equilibria, the initial state is relaxed under the influence of viscous and (possibly) resistive dissipation. The pressure is equilibrated along the magnetic field with the "artificial sound" [6] method. The method accelerates the equilibration by raising the effective sound speed to the Alfvén speed. Pressure is advanced by both advection and "artificial sound" to relax towards a state with

$$\mathbf{B} \cdot \nabla p = 0, \tag{1}$$

where $\mathbf{B}$ is the magnetic field and p is the pressure.

The kinetic energy is removed by viscous damping. Equilibria have been obtained for the proposed NCSX compact quasi-axisymmetric (QAS) stellarator [7], li383. Simulations are done with a fixed conducting wall boundary condition. They can be done of a single period or the whole torus. M3D equilibria agree well with VMEC, except that M3D magnetic fields can contain islands.

The equilibria have "stellarator symmetry." Linearization is possible by breaking the equilibrium symmetry. The symmetry angles are

$$\phi_{sym} = 0, \frac{\pi}{N_F}, \frac{2\pi}{N_F}, ...$$

where N_F is the number of equilibrium toroidal field periods. In NCSX, $N_F = 3$. Variables have the symmetry

$$f(R, Z, \phi_{sym} + \phi) = \pm f(R, -Z, \phi_{sym} - \phi). \tag{2}$$

In the symmetry planes, the variables $f = p, B_\phi, B_Z, v_R$ have up - down symmetry, with the plus sign, and the variables $f = B_R, v_Z, v_\phi$ have up - down anti symmetry, with the minus sign in (2). To linearize, perturbations can be applied with the opposite symmetry. This distinguishes between equilibrium and linear perturbations. Both equilibrium and stability

calculations can be performed in a single toroidal period, since most of the unstable modes of interest are short wavelength. The exceptions are TAE modes, which are calculated in the full torus. Linear and nonlinear simulations have been done of ideal and resistive instabilities. In Fig.1 is shown a pressure isosurface of a nonlinear ideally unstable ballooning mode, in the proposed NCSX design li383. The pressure perturbations follow the magnetic field, with maximum amplitude on the outside of the torus, and minimum amplitude on the inside.

In the proposed NCSX experiment, the li 383 design was found by a ballooning code, based on the short wavelength limit, to have a critical $\beta_c = 4.2\%$ At that β, the equilibrium was found to be unstable only in a thin edge region. Calculations with Terpsichore [8] found that β was limited by the external kink mode, with $\beta_c = 4\%$. The external kink is actually a kind of peeling mode, with moderate toroidal mode number n. At present, M3D can only simulate internal modes, but later it is planned to add a vacuum region, be modeled by high resistivity. The M3D ideal simulations, with no vacuum region, and moderate $n \approx 10$, were done at a resolution of 32 toroidal planes per period, with about 200 poloidal points on the boundary, and 50 radial points (5000 points in each poloidal plane $\times$ 32 planes = 160,000 mesh points). Linearization was done by imposing perturbations with anti - stellarator symmetry. The critical β was found to be $\beta_c \approx 6.5\%$. Hence β_c converges slowly with n. A similar finding that β_c for onset of moderate n modes is significantly higher than the β_c of the short wavelength ballooning limit has been noted elsewhere [9]. In [10] it was shown specifically for the proposed NCSX configuration C82 that global high-n modes (n up to 22) produce a higher β limit than the local ballooning results. The growth rate of the ideal modes is shown in the rightmost curve in Fig.2.

III. Resistive Stability

With nonzero resistivity, the moderate wavelength modes become resistive ballooning modes, which are unstable for almost all values of β. Fig.2 shows growth rate as a function of β. The leftmost curve is for modes with dimensionless resistivity $\eta = 1/S = 1.25\ 10^4$, and the rightmost curve is with zero resistivity. The resistive ballooning modes are similar in structure to ideal MHD ballooning modes, with a dispersion relation like tearing modes [11].

For perpendicular viscosity $\mu > \eta$ the growth rate scales as

$$\gamma \sim \eta^{5/6}. \tag{3}$$

This scaling was verified in M3D simulations, with $\eta \geq 10^4$. For smaller η, the scaling makes a transition to the viscous resistive interchange,

$$\gamma \sim \eta^{2/3}$$

This has not yet been verified numerically. It is known that the li383 equilibrium is resistive interchange unstable.

It is important to allow for resistive relaxation of equilibria, in order to allow the self consistent development of magnetic islands and magnetic stochasticity. Resistive ballooning modes limit the relaxation to a resistive steady state. It is helpful to take advantage of the

viscous tearing $\eta^{5/6}$ scaling. This permits relaxation for longer times before the modes grow too large. It is preferable to rely on two fluid effects to stabilize the modes, in order to obtain resistive equilibria.

IV. Two Fluid Stabilization

Most stellarators are resistive ballooning and resistive interchange unstable, yet it seems to have little effect experimentally. This suggests that some other physical effect is stabilizing the resistive modes. The simplest system that allows the electron and ion species to move separately is two fluids (electron and ion fluid equations). The two fluid terms are proportional to the Hall parameter,

$$H = \frac{c}{\omega_{pi} R}$$

where c/ω_{pi} is the ion skin depth and R is the major radius. In the simulations, $H = 0.01$ which is comparable to the expected experimental value. We use a nonlinear drift formulation of the two fluid equations similar to the Braginski equations [12]. The following calculations were done with the gyroviscous term only, neglecting the electron pressure,

$$\mathbf{E} + \mathbf{v} \times \mathbf{B} = \eta \mathbf{J} \tag{4}$$

$$\frac{\partial \mathbf{v}}{\partial t} + (\mathbf{v} \cdot \nabla)\mathbf{v} = -H \left(\mathbf{v}_{*i} \cdot \nabla\right) \mathbf{v}_{\perp} + \frac{\mathbf{J} \times \mathbf{B}}{\rho} - \frac{\nabla p}{\rho} \tag{5}$$

$$\mathbf{v}_{*i} = \mathbf{B} \times \nabla p_i / (H e n_i B^2). \tag{6}$$

where $\mathbf{E}$ is the electric field, $\mathbf{v}$ is the fluid velocity, $\mathbf{J}$ is the current density, ρ is the mass density, $p_i = p$ is the ion pressure, e is the electric charge, n_i is the ion number density, and $\mathbf{v}_{*i}$ is the ion drift velocity. The Hall term does not appear explicitly in Ohm's Law (4), as it would if the equations were expressed in terms of the ion velocity $\mathbf{v}_i$ [12]. We also took a constant density. An example computation in Fig.3, compares two nonlinear resistive calculations, one with $H = 0$, and one with $H = 0.01$, both with $S = 2000$, for an equilibrium with $\beta = 4\%$. The figure shows the electrostatic potential in the two cases, at the same time in their evolution from the initial state. The purely resistive case is quite unstable, and the electrostatic potential contains the flow cells on the outer edge of the plasma, typical of ballooning modes. The two fluid resistive case is stable, with a large scale flow pattern, which continues to evolve on a slow timescale. The calculation is nonlinear, so the perturbations in the purely resistive case have grown to finite amplitude. The value of S is unrealistically large, so the growth rate is also too large, but the mode is still stabilized with a realistic value of H. This suggests that finite H should be very effective in suppressing resistive ballooning and interchange modes. The simulations do not determine whether the modes are completely stable or simply slowed down. Nor are the important electron pressure terms included. Future work will address these issues.

The effectiveness of the stabilization suggests that diamagnetic drift of the equilibrium could stabilize MHD modes. The diamagnetic drift frequency, ω_*, in units of the Alfvén time $\tau_A = R/v_A$, is

$$\omega_* \tau_A = nH\left(\frac{\beta_p a}{2qL_p}\right), \tag{7}$$

where β_p is the poloidal β, a is the minor radius, L_p is the pressure scale length, and q is the rotational transform. The quantity multiplying nH is of order unity. If $H = 0.01$ and $n = 10$ then $\omega_* \tau_A = 0.1$, which can be sufficient to stabilize ideal modes. This could have a large effect on the critical β for instability.

When the resistive modes can be stabilized by diamagnetic drifts, it is possible to consider resistive evolution of the equilibrium. In Fig.4 are field line traces at the same time in their evolution, for the same NCSX case as previously. In Fig.4(a), the field lines are stochastic in the outer region because of the resistive instability. In Fig.4(b), the field lines are closed. In this case a large island, with poloidal / toroidal mode numbers 5/3, is present. This is consistent with PIES [13] results.

V. Hot Particle Effects on Global Shear Alfvén Modes

M3D has an option to include a population of gyrokinetic hot ions, which are coupled to the bulk plasma fluid through their contribution to the pressure tensor in the momentum evolution equation,

$$\rho \frac{d\mathbf{v}}{dt} = -\nabla p - (\nabla \cdot \mathbf{P}_h)_\perp + \mathbf{J} \times \mathbf{B} \tag{8}$$

where $\mathbf{P}_h$ is calculated from the hot ion distribution, while the other quantities are calculated from the bulk plasma fluid.

A δf method is used for noise reduction. The particles are pushed on same mesh as the fluid. The main problem is to locate particles on the unstructured mesh. This has already been solved for field line tracing. The method is to search the neighborhood of a particle's previous location, to find the cell in which the particle is located. Once this is done, it is possible to interpolate the force to the particle location, and to accumulate the pressure tensor on the mesh. The hybrid method has been implemented for shared memory and distributed memory computers. In the distributed memory, massively parallel version, there is an additional complication of moving particles between processors, when particles exit the spatial domain contained in a processor.

We look for TAE [14] modes in a $N_F = 2$ period QAS stellarator equilibrium. We choose a q profile favorable for TAE modes in tokamaks, with

$$2.4 < q < 2.9$$

or, ι varying from 0.417 at the magnetic axis to 0.345 at the edge.

This gives a TAE continuum gap at $q = 2.5$. The equilibrium has $R/a = 4$ and $\beta = 0.014$. The hot ions have a slowing - down distribution with Larmor radius $\rho_{fast}/a = 0.12$, and speed $v_{fast}/v_A = 1.6$. Unlike the ballooning modes, the TAE modes are long wavelength. We linearize by adding $n = 1$ perturbations to break the equilibrium symmetry, then letting the unstable modes grow. We can identify the unstable modes from their frequency and growth rates. We find the frequency

$$\omega = v_A/(2qR)$$

with $q = 2.5$. The growth rate is linear in hot particle β_h, as shown in Fig.5. It is possible to produce a sequence of equilibria varying smoothly between a stellarator and a tokamak,

by diminishing the amplitude of the 3D perturbations of the outer boundary, while keeping the q and p profiles fixed. This is done by expressing the boundary flux surface in the form

$$\begin{aligned} R(\theta,\phi) &= \overline{R}(\theta) + \alpha\hat{R}(\theta,\phi) \\ Z(\theta,\phi) &= \overline{Z}(\theta) + \alpha\hat{Z}(\theta,\phi) \end{aligned} \tag{9}$$

where the ϕ average of $\hat{R}, \hat{Z} = 0$, and α is varied from 0 to 1. We find that 3 D geometry is stabilizing for this case, shown in Fig.6, where the horizontal axis is α. The growth rate decreases as we interpolate between tokamak and stellarator geometry. In Fig.7, is shown the electrostatic potential of the TAE mode in tokamak and stellarator geometry.

VI. Conclusion

The M3D code has several levels of physics, which are applied to stellarators. Ideal MHD is used to calculate β limits. Ideal MHD β limits depend strongly on n, the toroidal mode number. Resistive MHD computations find moderate toroidal mode number unstable resistive ballooning modes, well below the ideal MHD β limit. Resistive MHD must be combined with two fluid effects. Two fluid ion diamagnetic drift has a stabilizing effect on the resistive ballooning modes. Hot particle kinetic effects are also included, to study TAE modes in stellarators. The TAE modes are confirmed by their frequency and linear scaling of growth rate with hot particle β. The growth rate in a two period stellarator is lower than in a tokamak with the same profiles and average boundary shaping.

References

1. PARK, W., BELOVA, E.V., FU, G.Y., TANG, X.Z., STRAUSS, H.R., SUGIYAMA, L.E., "Plasma Simulation Studies using Multilevel Physics Models" Phys. Plasmas **6** 1796 (1999).

2. SUGIYAMA, L.E., PARK, W., STRAUSS, H.R., HUDSON, S.R, STUTMAN, D., TANG, X.Z., Studies of Spherical Tori, Stellarators and Anisotropic Pressure with M3D, Nucl. Fusion (2001).

3. STRAUSS, H.R. and LONGCOPE, W., An Adaptive Finite Element Method for Magnetohydrodynamics, J. Comput. Phys. 147, 318 - 336 (1998).

4. BALAY, S., GROPP, W.D., CURFMAN MCINNES, L., and SMITH, B.F., http://www.mcs.anl.gov/petsc (2000).

5. HIRSHMAN, S.P., WHITSON, J.C., "Steepest-descent moment method for three-dimensional magnetohydrodynamic equilibria," Phys. Fluids **26** 3553 (1983).

6. PARK, W., MONTICELLO, D., STRAUSS, H., MANICKAM, Phys. Fluids **29** (1986) 1171.

7. REIMAN, A. H., KU, L., MONTICELLO, D. A., et al., "Recent advances in the design of quasi-axisymmetric stellarator plasma configurations, Phys. Plasma **8** (2001) 2083.

8. ANDERSON, D. V., COOPER, W. A., GRUBER, R., MERAZZI, S., and SCHWENN, U., Scient. Comp. Supercomputer II, 159 (1990).

9. GARABEDIAN, P. R. "Three-dimensional tokamak equilibria and stellarators with two-dimensional magnetic symmetry, Plasma Phys. Control. Fusion **39** (1997) B129-B134.

10. FU, G. Y. *et al.*, 18th IAEA Fusion Energy Conference, Sorrento, Italy, 4-10 October 2000 (IAEA, Vienna) paper TH3/2.

11. STRAUSS, H.R., "Resistive ballooning modes," Phys. Fluids **24** (1981) 2004.

12. SUGIYAMA, L.E., and PARK, W., "A nonlinear two-fluid model for toroidal plasmas," Phys. Plasma **7** (2000) 4644.

13. HUDSON, S. R., MONTICELLO, D. A., and REIMAN, A. H., "Reduction of islands in full-pressure stellarator equilibria," Phys. Plasma **8** (2001) 3377.

14. FU, G. Y., and PARK, W., Phys. Rev. Lett. **74** (1995) 1594.

Figures

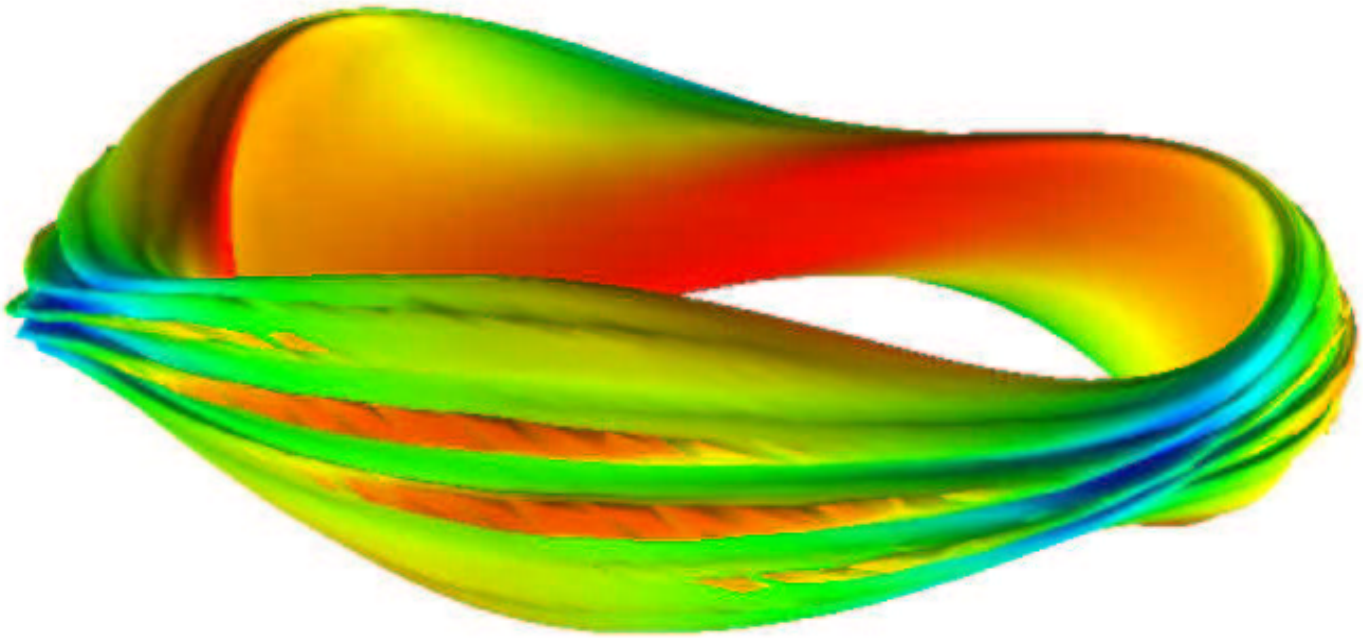

Figure 1: Pressure isosurface formed by nonlinear ballooning mode.

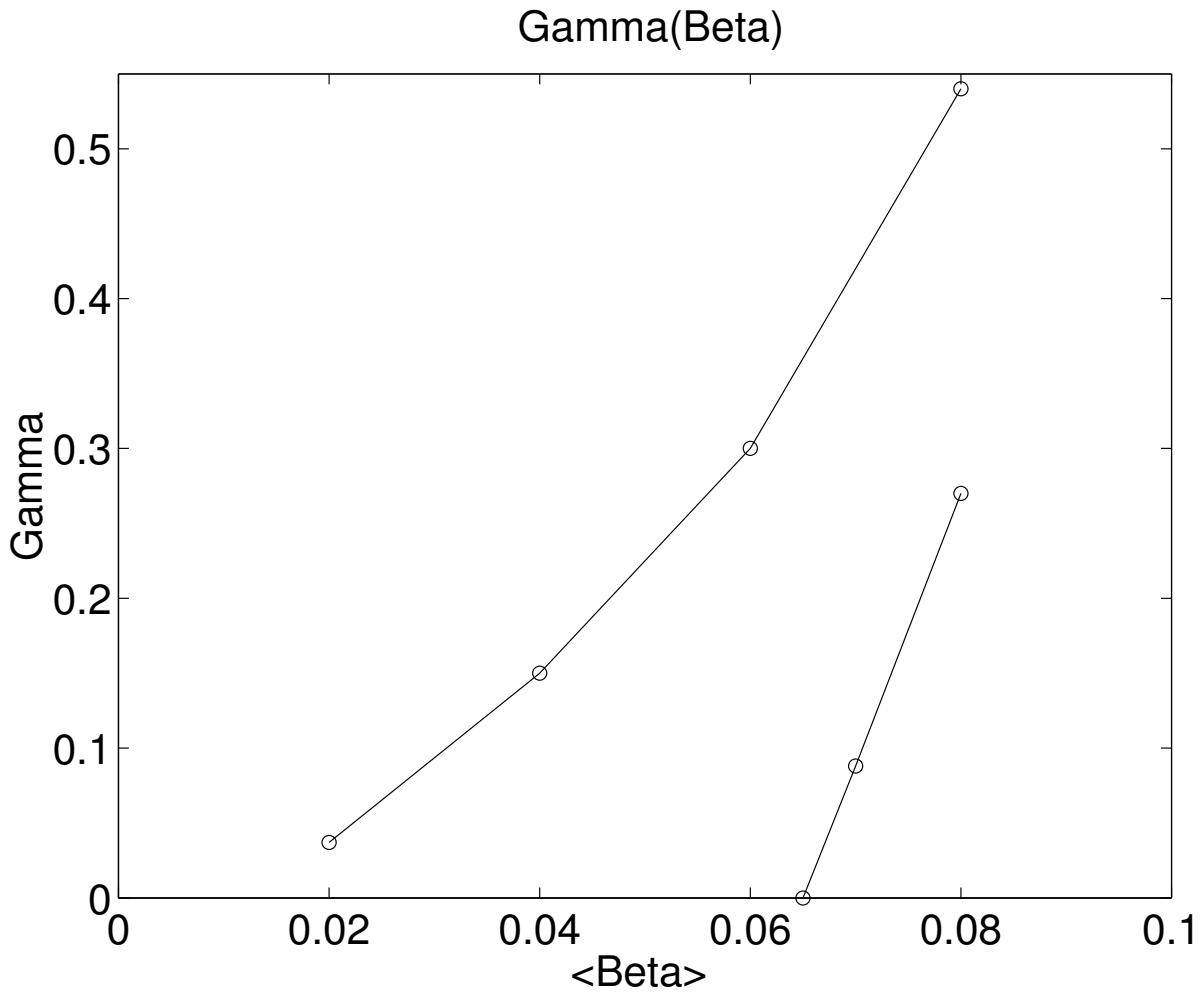

Figure 2: Growth rate γ of ideal and resistive modes vs. β

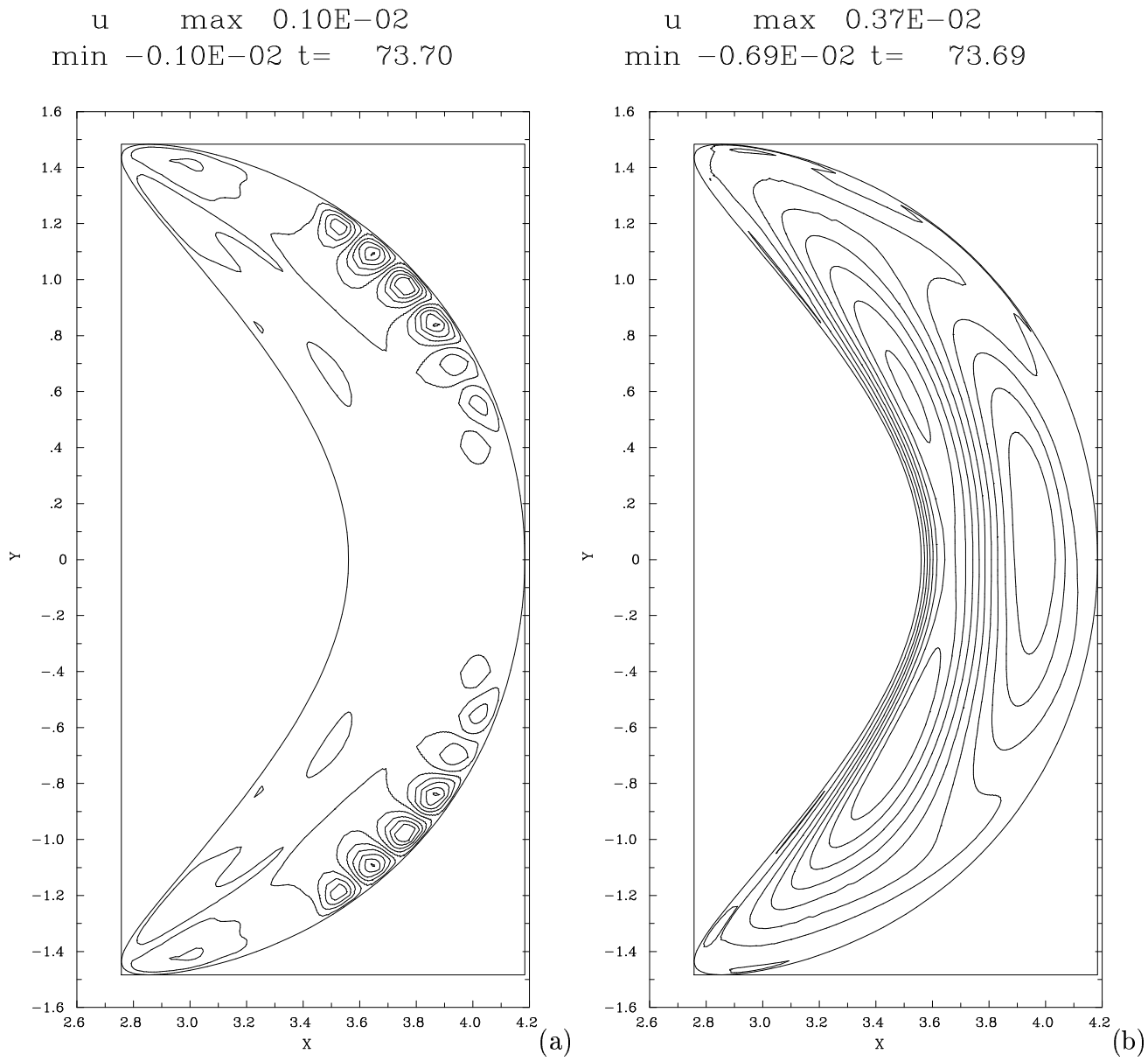

Figure 3: Electrostatic potential (a) resistive MHD, (b) 2 Fluid

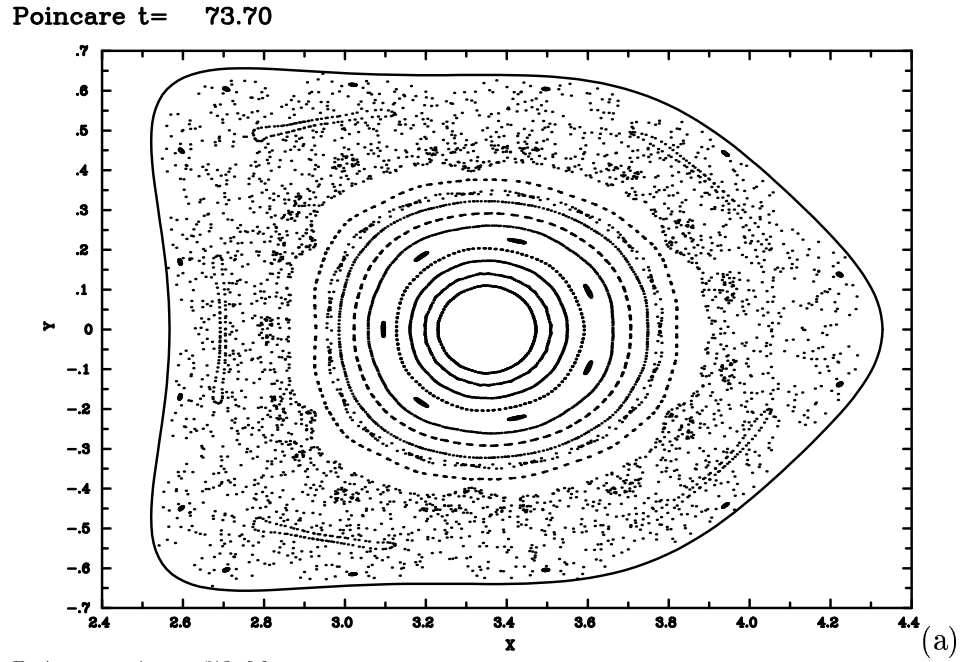

Figure 4: (a). Poincaré plot for MHD (b) 2 Fluid

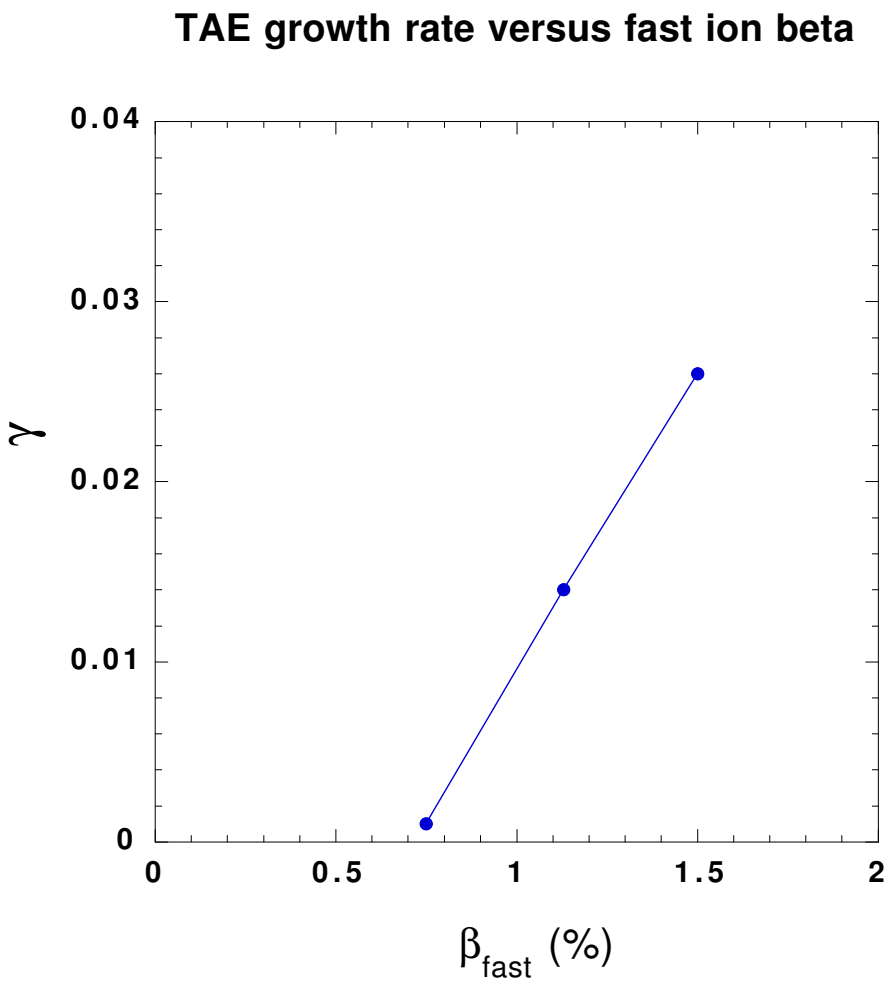

Figure 5: Growth rate γ vs. hot particle β.

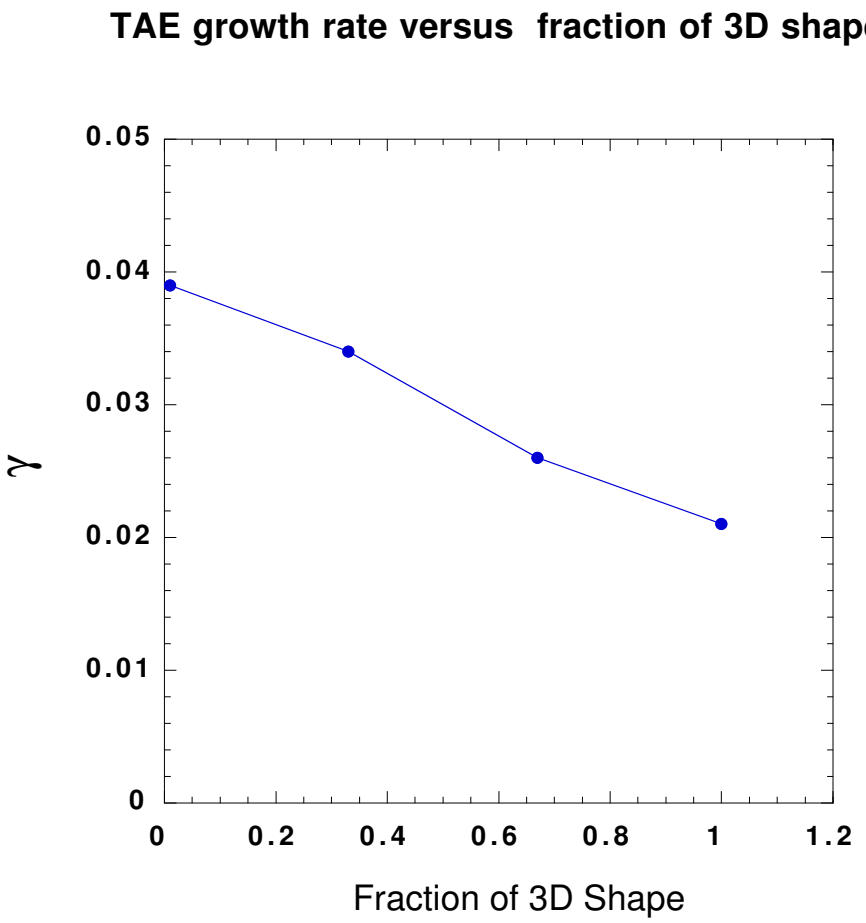

Figure 6: Growth rate γ vs. 3D shape for equilibria varying from tokamak to stellarator.

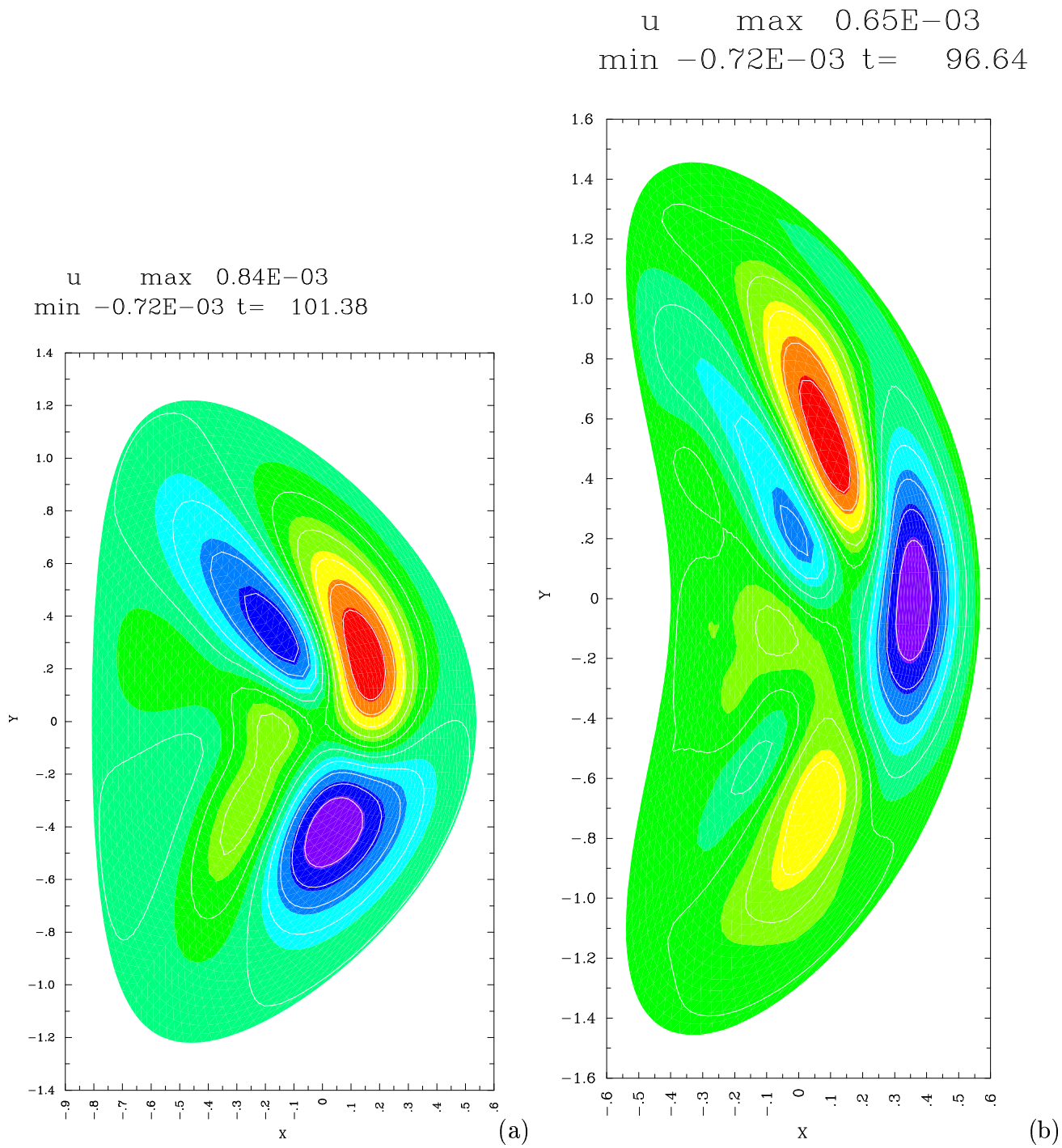

Figure 7: Electrostatic potential of TAE mode in (a) tokamak, (b) stellarator